Excitation of nonradiative surface-plasmon-polariton beams in nanoparticle arrays

T. D. Backes and D. S. Citrin
School of Electrical and Computer Engineering, Georgia Institute of Technology, Atlanta, Georgia 30332-0250, USA
(Received 8 August 2008; published 23 October 2008)

Gaussian beams of surface-plasmon polaritons in suitably designed two-dimensional square-lattice arrays of noncontacting noble-metal nanoparticles can be produced upon near-field optical excitation. Both positive- and negative-refraction effects are possible in the same structure and can be accessed simply by switching the polarization.

DOI: 10.1103/PhysRevB.78.153407 PACS number(s): 78.67.Pt, 73.20.Mf, 78.20.Ci, 78.67.Bf

Recently, Smolyaninov *et al.*[1,2] exploited surface-plasmon-(SP) polariton (SPP) optics on a metal film to show imaging with nanoscale resolution. While controversy concerning the analysis of the experiments persists,[3] this capability may rely on the large effective index of SPPs. Here we discuss a possible alternative approach to SPP optics based on suitably designed two-dimensional (2D) square-lattice (SL) nanoparticle arrays (NPA).[4] The use of a discrete periodic structure enables a variety of possibilities not afforded by a continuous metal slab or film in part because NPAs support excitations with dipole moment in the direction of the in-plane wave vector $\mathbf{q}$, i.e., of longitudinal (L) character. In addition, modes polarized transverse (T) with respect to $\mathbf{q}$ tend to exhibit dispersion in which the phase and group velocities $\mathbf{v}_g$ are of opposite sign; this is of intense interest for negative-refraction effects. While the use of gratings to launch SPPs is well known,[2,5,6] in the present case, the grating itself is used to engineer the SPPs in a way hitherto not suggested to our knowledge.

Central to this study, for 2D NPAs[7] with parameters chosen such that the SPPs for all $\mathbf{q}$ are radiative (subject to being diffracted out of plane) except for a very small range of values close to M in the SL Brillouin zone (BZ), near-field excitation can lead to the formation of Gaussian SPP beams with well-defined wave vector and transverse spatial extent. These beams can be associated with SPPs with group and phase velocities of the same or opposite signs depending largely on the direction of the SPP dipole moment with respect to $\mathbf{q}$. The focuses here are such beams and their flexibility for applications in photonics. Note that the formation of these beams is crucially dependent on the discrete and anisotropic structure due to the NPA and do not exist in films.

We use the coupled-dipole model.[8–10] Consider a SL 2D NPA of nanoparticles (NPs) of diameter δ and nearest-neighbor spacing d. If $d \gtrsim 1.25\delta$, the electric dipole dominates the optical properties,[11] enabling us to dispense with higher multipole moments. We assume spherical, isotropic NPs and work in the polarization basis X, Y, and Z with Z dipole moment in the direction normal to the NPA plane and X and Y dipole moment along principle axes x and y of the SL. The Z polarization results in transverse-electric SPPs, while the X and Y polarizations are coupled for general $\mathbf{q}$. We will also use the polarization basis for in-plane modes that are transverse T or longitudinal L with respect to $\mathbf{q}$; T and L are decoupled along ΓX and ΓM due to symmetry.

Before considering the electromagnetic modes of NPAs—the SPPs—we comment here on the central role of loss or, from the propagation standpoint, attenuation, of which there are two main sources. First, there is radiative damping as the energy stored in the SP is radiated into the far field. Second, there is nonradiative damping. Provided the NPs are not too small [$\gtrsim 5$ nm (Ref. 12)], the single-NP SP is damped due to the imaginary part of the bulk metal dielectric constant, i.e., due to high-frequency resistive loss. The dominant source of loss in single NPs is typically nonradiative loss,[13] and it is further suspected that this is also the case in most NP chains[14] and NPAs to date. In a NP chain or NPA, however, small-$\mathbf{q}$ modes can have much higher radiative-decay rates than for single NPs due to the constructive interference between the radiations from the various NPs in the far field. In fact, the characteristic decay rate, as well as the spectral bandwidth of SPPs for a NP chain or NPA, scales as d^{-3}; hence, there is promise to produce structures in which *radiative* effects dominate despite the substantial nonradiative losses in single NPs. While this is not the prevailing state of affairs in current structures, it is reasonable to expect that this situation might be reversed in the near future with improvements in structure fabrication. In the following, therefore, to concentrate on the effects predicted here, we assume that radiative effects dominate over nonradiative losses.

The SPPs correspond to the resonances of the Green's function (GF) $G_\alpha(\mathbf{q},\varepsilon)$, where α indicates the mode. For the periodic NPA, a SPP at $\mathbf{q}$ does not undergo scattering to $\mathbf{q}' \neq \mathbf{q}$; hence, $G_\alpha^{-1}(\mathbf{q},\varepsilon)\delta_{\mathbf{q}\mathbf{q}'} = [G_0^{-1}(\varepsilon) - \Sigma_0 - \Sigma_\alpha(\mathbf{q},\varepsilon)]\delta_{\mathbf{q}\mathbf{q}'}$ with $G_0^{-1}(\varepsilon) = (\varepsilon^2 - \varepsilon_p^2 - i\gamma_p)/(2\varepsilon_p)$ the single-NP-SP GF. The radiative self-energy (SE) is $\Sigma_\alpha(\mathbf{q},\varepsilon) = \Sigma'^{\infty}_{h,j=-\infty}\Sigma_{h,j;\alpha}(\varepsilon)e^{i(q_x hd + q_y jd)}$, where ε_p and γ_p are the energy and nonradiative damping of the single-NP SP resonance and the prime on the summation means that term $(h,j)=(0,0)$ is to be omitted. We assume $\gamma_p = 0$ to focus on diffractive effects. Diffractive (radiative) losses out of the plane originate from $-2\ \mathrm{Im}\ \Sigma_0/\hbar$, which is the radiative-decay rate of a single-NP SP. The real and imaginary parts of the divergences of $G_\alpha(\mathbf{q},\varepsilon)$ give the SPP dispersion energy and the diffractive decay rate. Note that although the labels are omitted above, the SE is a matrix in the polarization indices X, Y, (or L, T) and Z,[10] as discussed further below.

The SE is the dipole-dipole energy of NP's (h,j) and (h',j'), i.e., $\Sigma_{(h,j)-(h',j')}(\varepsilon) = \mathbf{E}_{(h,j),(h',j')} \cdot \mathbf{p}_{(h',j')}$ with $\mathbf{E}_{(h,j),(h',j')}$ the oscillating [as $\exp(-i\omega t)$] electric field at the location of NP (h',j') associated with NP (h,j), while $\mathbf{p}_{(h',j')}$ is the dipole moment of the SP of NP (h',j'); the full ex-

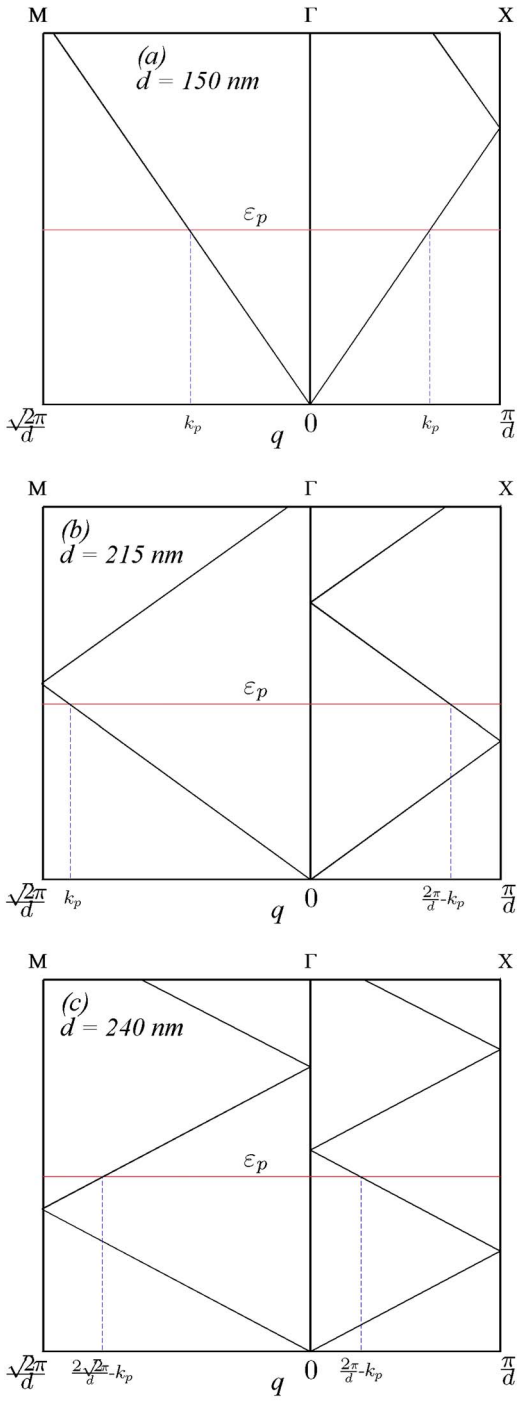

FIG. 1. (Color online) Photon and SPP dispersion for $\mathbf{q}$ along ΓX and ΓM for (a) $d=150$ nm, (b) $d=215$ nm, and (c) $d=240$ nm.

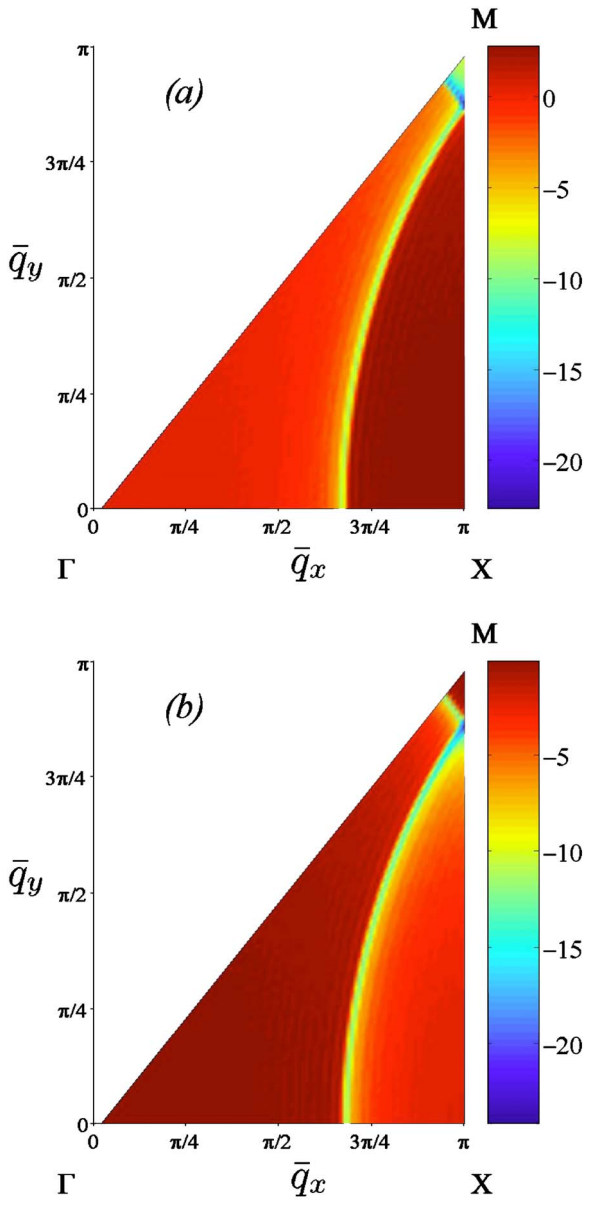

FIG. 2. (Color online) (a) Z SPP dispersion Re $\sigma(\bar{\mathbf{q}},\bar{k})$ and (b) radiative width $-$Im $\sigma(\bar{\mathbf{q}},\bar{k})$ for a Au $\delta=50$-nm square-lattice NPA with $d=215$ nm.

pression is lengthy and is given in Ref. 9. In general, Z is decoupled from X and Y (or L and T); the in-plane-polarized modes are thus obtained from the upper 2×2 block. The intra-NP SE is $\Sigma_0 \approx -\frac{2}{3}i\gamma = -\frac{2}{3}in\gamma_0$ with $2\frac{2}{3}\gamma_0/\hbar$ the radiative-decay rate in the absence of the medium with index n; $2\gamma_0/\hbar$ is the single-NP radiative-decay rate. We normalize energies to γ_0 as $\underline{\underline{\sigma}}(\bar{\mathbf{q}},\bar{k}) = \gamma_0^{-1}\underline{\underline{\Sigma}}(\mathbf{q},\varepsilon)$ (here expressed in matrix form), where $\bar{k}=kd$, $\bar{\mathbf{q}}=\mathbf{q}d$, and $k=\omega\epsilon^{1/2}/c$ the optical wave vector in the background medium with $\sqrt{\epsilon}$ the background refractive index and $\hbar\omega=\varepsilon$. We consider a NPA of $\delta=50$-nm Au NPs (Ref. 14), where $\hbar/(2\gamma_0)$ is a few fs and on the order of nonradiative dephasing $\hbar/(2\gamma_p)$.[13,15] We take the embedding medium as low loss with Re $n=3.5$ and Im $n=0.01$, and account for the effect of the background index on the NP SP resonance via $\varepsilon_p=(\varepsilon_p)_{\text{air}}/(\frac{2}{3}+\frac{1}{3}\text{Re}\, n)$ (Ref. 15) with $(\varepsilon_p)_{\text{air}}=2$ eV (Refs. 13 and 14) the single-NP SP resonance in air with $k_p=\varepsilon_p \text{Re}\, n/\hbar c$.

The modes are found by finding the resonances as a function of ε of the eigenvalues of $\underline{\underline{G}}^{-1}(\mathbf{q},\varepsilon)$ at each $\mathbf{q}$. These resonances are of two types depending on whether the magnitude q of the wave vector $\mathbf{q}$ satisfies $q<\varepsilon$ Re $n/\hbar c$ (inside the light line) or $q>\varepsilon$ Re $n/\hbar c$ (outside the light line). (Roughly speaking, because we do not know *a priori* the

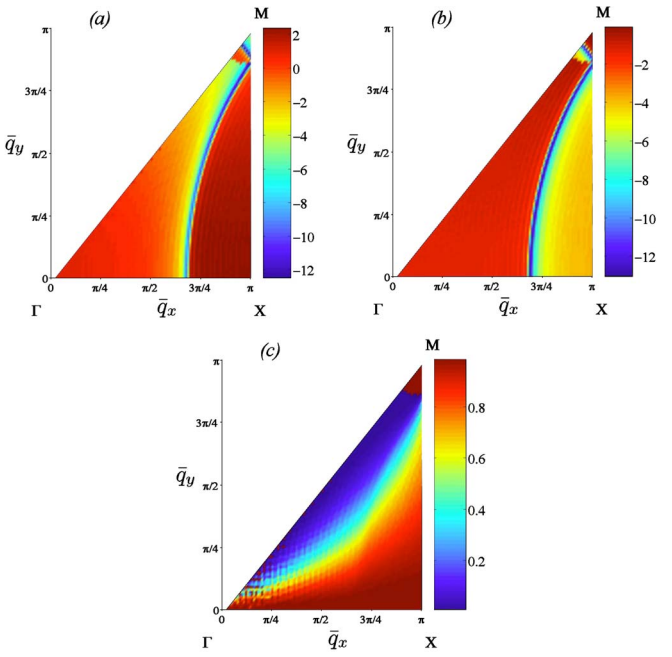

FIG. 3. (Color online) (a) First of two in-plane polarized SPP dispersion Re $\sigma(\bar{\mathbf{q}},\bar{k})$ and (b) radiative width $-\mathrm{Im}\,\sigma(\bar{\mathbf{q}},\bar{k})$ for a Au δ=50-nm square-lattice NPA with d=215 nm. (c) Transverse component of the eigenvector for this in-plane SPP.

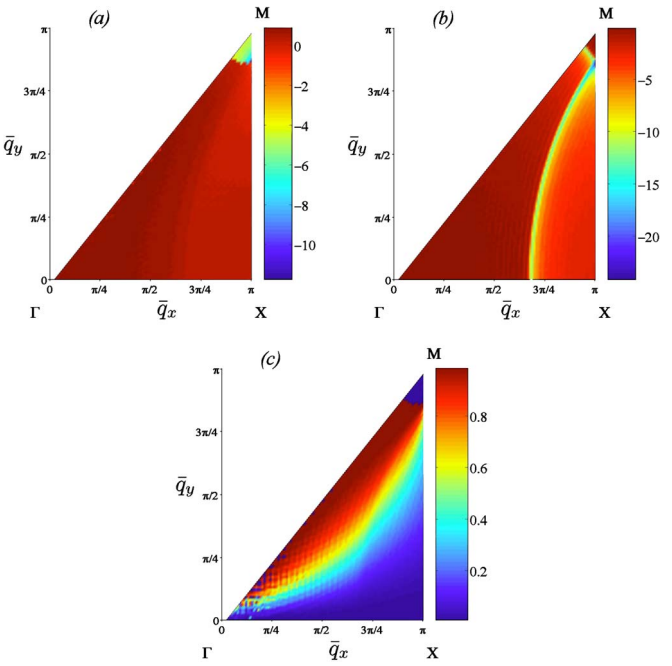

FIG. 4. (Color online) (a) Second of two in-plane polarized SPP dispersion Re $\sigma(\bar{\mathbf{q}},\bar{k})$ and (b) radiative width $-\mathrm{Im}\,\sigma(\bar{\mathbf{q}},\bar{k})$ for a Au δ=50-nm square-lattice NPA with d=215 nm. (c) Transverse component of the eigenvector for this in-plane SPP.

energy of the resonance, we can in practice replace ε Re $n/\hbar c$ above by $k_p=\varepsilon_p$ Re $n/\hbar c$.) Neglecting any nonradiative loss (as well as Im n), modes with $q<k_p$ are subject to radiative decay. That is, there exist resonant far-field photons whose in-plane wave vector $\mathbf{q}$ and component in the Z direction is real. For $q<k_p$, however, no such resonant far-field photons exist that enable decay while obeying energy and momentum conservation. In this latter case, the modes are said to be SPPs, as the electromagnetic component associated with the mode is evanescent away from the NPA.

Figure 1 shows how the parameters can lead to SPP beam forming. Shown is the photon and SPP dispersion for $\mathbf{q}$ along ΓX and ΓM, omitting the coupling between the SP and photon field for (a) d=150 nm, (b) 215 nm, and (c) 240 nm. For (a), the photon dispersion is not zone folded along any direction by the time it crosses the SP dispersion (at ε_p), i.e., $k_p<\pi/d, \sqrt{2}\pi/d$. SPPs that are formed when the SPs and photons are coupled, leading to hybrid modes outside the light line that cannot undergo radiative decay. For (b), $\pi/d<k_p<\sqrt{2}\pi/d$, and the crossing ΓX occurs after the photon dispersion has undergone zone folding; all SPPs along ΓX are radiative, as shown in Ref. 16. Along ΓM, the crossing occurs very shortly before zone folding. There is a small region near M where the SPPs are nonradiative, leading to beam forming. The effect of increasing d is shown in Fig. 1(c); $\pi/d, \sqrt{2}\pi/d<k_p$ so that the crossing in all cases occurs after zone folding of the photon dispersion has occurred. Here, all SPPs are subject to diffractive loss.

Now allow for coupling between the SP and photon dispersion with d=215 nm in Figs. 2–4. One sees a small region close to M where the SP-like SPPs are nonradiative; elsewhere they are subject to diffractive loss. The two in-plane modes $\pm$ have highly mixed T and L characters, depending on $\bar{q}$. The first "+" is dominantly L along ΓM and T along ΓX. The other "−" shows the opposite behavior.

How can we understand the formation of well-defined SPP beams in which k_p is just greater than $\sqrt{2}\pi/d$? For clarity, we consider the excitation of a single NP at ε and compute the SP amplitude $F(\mathbf{r})$ on NP at position $\mathbf{r}$ with $r \gg d$. We assume that the near-field excitation contains spatial-frequency components of a single polarization ($\pm$ or Z). (This may be achieved possibly by the use of optical vector beams[17] with an appropriate near-field excitation source.) We leave out nonradiative decay that tends to attenuate the SPPs. Thus our treatment suggests limiting behavior expected where nonradiative attenuation can be suppressed. In the large-r limit, only nonradiative lower-branch SPPs contribute since radiative modes will be attenuated by diffraction prior to arriving at a distant point $\mathbf{r}$. Thus,

$$F(\mathbf{r}) = \lim_{r\to\infty} \sum_{\mathbf{q}} G(\mathbf{q},\varepsilon + i0^+)e^{i\mathbf{q}\cdot\mathbf{r}}$$
$$= \left(\frac{L}{2\pi}\right)^2 \lim_{r\to\infty} \int_{\mathrm{BZ}} d^2q G(\mathbf{q},\varepsilon + i0^+)e^{i\mathbf{q}\cdot\mathbf{r}}$$
$$= \frac{L^2}{2\pi}\int_{\mathrm{BZ}} d^2q\,\delta(\varepsilon - \varepsilon_{\mathbf{q}})e^{i\mathbf{q}\cdot\mathbf{r}} \qquad (1)$$

with L^2 the normalization area and $G^{-1}(\mathbf{q},\varepsilon)=\varepsilon-\varepsilon_{\mathbf{q}}=\varepsilon-\varepsilon_p-\Sigma(\varepsilon,\mathbf{q})$. Arguments of the δ function are limited to $\mathbf{q}$ with $\mathbf{v}_g\cdot\mathbf{r}>0$ and $G^{-1}(\mathbf{q},\varepsilon+i0^+)=0$ with $\varepsilon_{\mathbf{q}}\in\mathbb{R}$. We treat the case when the resonant SPPs have projection of group and phase velocities positive $\mathbf{v}_g\cdot\mathbf{q}>0$ and the case when $\mathbf{v}_g\cdot\mathbf{q}<0$. The

first (second) case is given by the upper (lower) signs below. By considering an optical axis along ΓM, and retaining phase-front curvature up to second order, one finds $F(\mathbf{r}) = \rho_n(\varepsilon)\frac{1}{2\pi}\sqrt{\frac{\pi}{\beta_\pm}}e^{\pm iq_\varepsilon\zeta}e^{\pm iq_\varepsilon/2\zeta\xi^2}e^{-\xi^2/\chi^2\zeta^2}$ with $\rho_n(\varepsilon)$ the partial density of nonradiative SPP states, q_ε the value of q where $\varepsilon-\varepsilon_q=0$, $\frac{\pi}{4}-\chi<\phi<\frac{\pi}{4}+\chi$ with $\chi\ll 1$ so that $\varepsilon-\varepsilon_\mathbf{q}=0$ defines the range of angles near M with nonradiative SPPs, ζ the distance along the optical axis ΓM, ξ the distance in the NPA plane perpendicular to the ζ axis, and $\beta_\pm = \chi^{-2} \pm iq_\varepsilon\zeta/2$.

Thus, an excitation at large r only occurs if there is a density of nonradiative SPPs $\rho_n(\varepsilon)$ at ε. The radical is a phase and amplitude varying as $\sqrt{\mp 2\pi i/(q_\varepsilon\zeta)}$ for large ζ; $\exp(\pm iq_\varepsilon\zeta)$ is the phase of a wave of wave vector q_ε along ζ; the upper (lower) sign is for the case where the projection of the group and phase velocities is positive (negative); $e^{\pm iq_\varepsilon\xi^2/(2\zeta)}$ describes the quadratic phase of a circular wave with source at the origin. For $\mathbf{v}_g\cdot\mathbf{q}<0$, the phase fronts are *converging* toward the origin for increasing ζ; $e^{-\xi^2/(\chi\zeta)^2}$ gives the transverse spatial extent $\chi\zeta$ of the beam increasing with ζ.

The proposed structure is also convenient to couple light in (or out) vertically. See Fig. 5 where a region of the NPA is fabricated from two types of NPs. By doubling the lattice constant to $2d$ in the region shown, and consequently folding the BZ, all SPPs here are radiative. Moreover, since the original structure with lattice constant d was designed in the first place so that only a very small region of the BZ near M are *not* subject to diffractive loss, the diffracted light that occurs in the tailored area is emitted essentially vertically. Similarly, such structures can be used to form SPP beams near M by coupling light in from the far field; the spatial extent of the tailored region can be used to determine that spatial width of the SPP beams that are formed, and thus a small tailored region, can serve as a near-field excitation source as well as a probe.

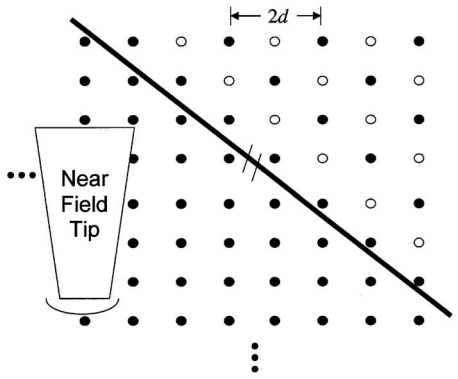

FIG. 5. Near-field excitation of a SL 2D NPA for beam forming. In the region in the upper right, the open dots indicate NPs different from those elsewhere in the NPA.

To conclude, we show for the 2D SL NPA, when $d \leq \sqrt{2}\pi/k_p$, there is a small area of $\mathbf{q}$ space close to M where the SP-like SPPs are nonradiative. For near-field excitation, these modes lead to the formation of well-defined beams not susceptible to diffractive losses in ΓM. Such beams, which have approximately quadratic phase fronts, possess distinct polarization-dependent behavior; the group and phase velocities can be in the same or opposite directions depending on the direction of the SP dipole moment. While many of these effects can also in principle be produced in purely dielectric-based photonic-crystal slabs, the use of metal-NP-based structures enables one to accomplish such effects in much thinner layers and also to achieve integration in ways that might not be possible with purely dielectric structures (such as plasmonic mirrors on semiconductor lasers). Moreover while NPAs suffer from significant nonradiative losses, future developments in nanofabrication may in part alleviate such difficulties.

[1] I. I. Smolyaninov, J. Elliott, A. V. Zayats, and C. C. Davis, Phys. Rev. Lett. **94**, 057401 (2005).
[2] I. I. Smolyaninov, C. C. Davis, J. Elliott, G. A. Wurtz, and A. V. Zayats, Phys. Rev. B **72**, 085442 (2005).
[3] A. Drezet, A. Hohenau, and J. R. Krenn, Phys. Rev. Lett. **98**, 209703 (2007); I. I. Smolyaninov, C. C. Davis, J. Elliott, and A. V. Zayats, *ibid.* **98**, 209704 (2007).
[4] M. Quinten, A. Leitner, J. R. Kren, and F. R. Aussenegg, Opt. Lett. **23**, 1331 (1998).
[5] T. W. Ebbesen, H. J. Lezec, H. F. Ghaemi, T. Thio, and P. A. Wolff, Nature (London) **391**, 667 (1998).
[6] Other far-field techniques beyond the Rayleigh criterion have been proposed. See, for example, A. Sentenac, P. C. Chaumet, and K. Belkebir, Phys. Rev. Lett. **97**, 243901 (2006).
[7] K. Sakoda, *Optical Properties of Photonic Crystals* (Springer, Berlin, 2001); S. Zou and G. C. Schatz, J. Chem. Phys. **121**, 12606 (2004).
[8] V. A. Markel, J. Mod. Opt. **40**, 2281 (1993); A. Alù and N. Engheta, Phys. Rev. B **74**, 205436 (2006).
[9] D. S. Citrin, Nano Lett. **4**, 1561 (2004); **5**, 985 (2005); **31**, 98 (2006); J. Opt. Soc. Am. B **22**, 1763 (2005).
[10] T. D. Backes and D. S. Citrin, IEEE J. Sel. Top. Quantum Electron. (to be published).
[11] S. Y. Park and D. G. Stroud, Phys. Rev. B **69**, 125418 (2004).
[12] T. V. Shahbazyan, I. E. Perakis, and J.-Y. Bigot, Phys. Rev. Lett. **81**, 3120 (1998); T. V. Shahbazyan and I. E. Perakis, Phys. Rev. B **60**, 9090 (1999); Chem. Phys. **251**, 37 (2000).
[13] C. Sönnichsen, T. Franzl, T. Wilk, G. von Plessen, J. Feldmann, O. Wilson, and P. Mulvaney, Phys. Rev. Lett. **88**, 077402 (2002); T. Klar, M. Perner, S. Grosse, G. von Plessen, W. Spirkl, and J. Feldmann, *ibid.* **80**, 4249 (1998).
[14] S. A. Meier, P. G. Kik, and H. A. Atwater, Appl. Phys. Lett. **81**, 1714 (2002).
[15] K. L. Kelly, E. Coronado, L. L. Zhao, and G. C. Schatz, J. Phys. Chem. **107**, 668 (2003).
[16] D. S. Citrin, Opt. Lett. **20**, 901 (1995).
[17] R. Dorn, S. Quabis, and G. Leuchs, Phys. Rev. Lett. **91**, 233901 (2003); K. C. Toussaint, Jr., S. Park, J. E. Jureller, and N. F. Scherer, Opt. Lett. **30**, 2846 (2005); A. Flores-Pérez, J. Hernández- Hernández, R. Jáuregui, and K. Volke-Sepúlveda, *ibid.* **31**, 1732 (2006).